NATIONAL ADVISORY COMMITTEE FOR AERONAUTICS

TECHNICAL NOTE 2122

THEORETICAL CALCULATIONS OF THE LATERAL FORCE AND YAWING MOMENT DUE TO ROLLING AT SUPERSONIC SPEEDS FOR SWEPTBACK TAPERED WINGS WITH STREAMWISE TIPS

SUBSONIC LEADING EDGES

By Kenneth Margolis

Langley Aeronautical Laboratory
Langley Air Force Base, Va.

Washington
June 1950

NATIONAL ADVISORY COMMITTEE FOR AERONAUTICS

TECHNICAL NOTE 2122

THEORETICAL CALCULATIONS OF THE LATERAL FORCE AND YAWING MOMENT DUE TO ROLLING AT SUPERSONIC SPEEDS FOR SWEPTBACK TAPERED WINGS WITH STREAMWISE TIPS

SUBSONIC LEADING EDGES

By Kenneth Margolis

SUMMARY

On the basis of linearized-supersonic-flow theory, the lateral force and yawing moment due to combined angle of attack and rolling have been evaluated for families of thin sweptback tapered wings with streamwise tips. Equations were derived for wings that are contained between the Mach cones springing from the wing apex and from the trailing edge of the root section, that is, wings with subsonic leading edges and supersonic trailing edges. Some calculations, based on these equations, are included for groups of wings with subsonic trailing edges.

Design charts are presented which permit estimation of the stability derivatives C_{Y_p} and C_{n_p} for given values of Mach number, aspect ratio, taper ratio, and leading-edge sweep. Some illustrative variations of the derivatives with these parameters are also included. All numerical data are presented relative to a body-axes system with moments taken about the wing apex. For convenience in application, formulas are given for transforming from this system to a stability-axes system with moments taken about an arbitrary point.

INTRODUCTION

A number of papers dealing with the theoretical calculations of stability derivatives at supersonic speeds have been published to date. Wing plan forms that have been treated in detail include the rectangular, trapezoidal, and triangular wings and modified forms of the triangular wing. (See, for example, references 1 to 10.) An important group of

plan forms for which only a few of the stability derivatives have been investigated consists of sweptback wings with streamwise tips. The lift-curve slope C_{L_α} and the damping-in-roll derivative C_{l_p} have been calculated for streamwise-tip wings and are presented in references 11 and 12. Other papers presenting calculations for this group of plan forms include references 13 to 15.

The present paper treats the lateral force and yawing moment due to combined angle of attack and rolling at supersonic speeds for sweptback tapered wings with streamwise tips and subsonic leading edges. (An edge is termed "subsonic" if the stream-flow component normal to the edge is subsonic, and is termed "supersonic" if the normal component is supersonic.) The analysis is based on an application of linearized theory and is therefore subject to all the usual restrictions and limitations. It is appropriate to point out that the degree of applicability of these derivatives to actual full-scale wings may be somewhat uncertain for the reasons (relative to suction-force evaluation) pointed out in reference 4 for triangular wings.

Results are given in the form of generalized equations for the stability derivatives C_{Y_p} and C_{n_p} together with a series of design curves from which estimates of the derivatives can be made for given values of aspect ratio, taper ratio, Mach number, and leading-edge sweep. For illustrative purposes, variations of the derivatives with these parameters for specific wing configurations are also presented.

SYMBOLS

x,y	Cartesian coordinates of an arbitrary point
V	flight speed
v_n	induced velocity normal to edge
s_n	perpendicular distance from edge
α	angle of attack
p,r	angular velocities about x- and z-axes, respectively
M	stream Mach number
M_n	Mach number of flow component normal to an edge
μ	Mach angle

B	cotangent of Mach angle $\left(\sqrt{M^2 - 1}\right)$
F	suction force
Y	lateral force
L'	rolling moment
N	yawing moment
Λ	sweepback angle of leading edge
$m = B \cot \Lambda$	
c_r	root chord
h	distance from wing apex to moment reference, root chords
λ	taper ratio (ratio of tip chord to root chord)
b	wing span
S	wing area
A	aspect ratio $\left(A = \frac{b^2}{S} = \frac{2b}{c_r(1 + \lambda)}\right)$
ω	geometric parameter of wing $\left(\omega = \frac{2c_r}{b} \cot \Lambda = \frac{4m}{AB(1 + \lambda)}\right)$
φ	velocity potential
ρ	density of air
C_l	rolling-moment coefficient $\left(\frac{L'}{\frac{1}{2}\rho V^2 Sb}\right)$
C_Y	lateral-force coefficient $\left(\frac{Y}{\frac{1}{2}\rho V^2 S}\right)$
C_n	yawing-moment coefficient $\left(\frac{N}{\frac{1}{2}\rho V^2 Sb}\right)$

$$C_{Y_p} = \left(\frac{\partial C_Y}{\partial \frac{pb}{2V}}\right)_{\frac{pb}{2V} \to 0}$$

$$C_{n_p} = \left(\frac{\partial C_n}{\partial \frac{pb}{2V}}\right)_{\frac{pb}{2V} \to 0}$$

$$C_{l_p} = \left(\frac{\partial C_l}{\partial \frac{pb}{2V}}\right)_{\frac{pb}{2V} \to 0}$$

$$C_{n_r} = \left(\frac{\partial C_n}{\partial \frac{rb}{2V}}\right)_{\frac{rb}{2V} \to 0}$$

$k = \sqrt{1 - m^2}$

$E\left(\sqrt{1 - m^2}\right)$ complete elliptic integral of second kind with modulus k

$$\left(\int_0^{\pi/2} \sqrt{1 - k^2 \sin^2 z}\, dz\right)$$

$F\left(\sqrt{1 - m^2}\right)$ complete elliptic integral of first kind with modulus k

$$\left(\int_0^{\pi/2} \frac{dz}{\sqrt{1 - k^2 \sin^2 z}}\right)$$

$$I(m) = \frac{2(1 - m^2)}{(2 - m^2)E\left(\sqrt{1 - m^2}\right) - m^2 F\left(\sqrt{1 - m^2}\right)}$$

$$J(m) = \frac{I(m)\sqrt{1 - m^2}}{E\left(\sqrt{1 - m^2}\right)}$$

Subscripts:

1,2	refer to leading edge and tip, respectively
α,p	refer to lift and roll, respectively
a	moments taken about wing apex
R,L	refer to right and left edges, respectively

All angles are measured in radians.

ANALYSIS

Scope

The basic sweptback wings considered in the present paper are sketched in figure 1. These wings have subsonic leading edges and supersonic trailing edges; an added restriction is that the Mach lines emanating from the wing tips may not intersect on the wing. Equations are derived herein for the lateral force and yawing moment due to combined angle of attack and rolling specifically for plan forms satisfying these limitations. These equations are utilized in extending the range of computations to include some plan forms with subsonic trailing edges. Application and interpretation of the results are subject to the inherent restrictions and limitations of the linearized-thin-airfoil theory of supersonic flow.

The orientation of the wing with respect to a body system of coordinate axes used in the analysis is indicated in figure 2(a). The surface velocity potentials used herein and the expressions for the stability derivatives are derived with respect to this system. All calculations for the derivatives C_{Y_p} and C_{n_p} are presented relative to this same system of body axes. For convenience, the moments are taken about the wing apex and are considered positive for clockwise rotation. Transformation equations are presented for moments taken about an arbitrary point and also for converting the derivatives to a stability-axes system. (See fig. 2(b) for orientation of stability axes.)

Basic Considerations

The lateral force and yawing moment due to rolling relative to body axes for a very thin wing without dihedral arise entirely from suction forces on the wing edges. For the general plan form under consideration,

these suction forces are along the leading edge and wing tip and may be evaluated by applying a method suggested in reference 16 for incompressible flow and modified for compressibility effects in reference 3. Thus, if the induced surface velocity normal to and in the immediate vicinity of a subsonic edge is expressed as

$$(v_n)_{s_n \to 0} = \pm \frac{G}{\sqrt{s_n}} \tag{1}$$

where s_n is the perpendicular distance from the edge and G is a constant, there results a suction force per unit length of edge

$$F = \pi \rho G^2 \sqrt{1 - M_n^2} \tag{2}$$

where M_n is the Mach number of the stream component normal to the edge.

An expression for the suction force per unit length of leading edge F_l which is directly applicable to the subsonic leading edge of the wing under consideration herein (see fig. 1) may be obtained from reference 4 and is as follows

$$F_l = \mp \frac{\pi}{2} \rho x \sqrt{1 - m^2} \cot \Lambda \left\{ \frac{\alpha^2 V^2}{\left[E\left(\sqrt{1 - m^2}\right) \right]^2} + \frac{\left[I(m) \right]^2 p^2 x^2 \cot^2 \Lambda}{4} \pm \frac{I(m) \alpha V p x \cot \Lambda}{E\left(\sqrt{1 - m^2}\right)} \right\} \tag{3}$$

where the plus sign is to be used for the right leading edge and the minus sign for the left leading edge.

An expression for the suction force along the wing tips must now be derived. Consider the induced surface velocity normal to the streamwise tip of a wing rolling with an initial angle of attack. This velocity is

$$v_{n_2} = \frac{\partial \varphi}{\partial y} = \left(\frac{\partial \varphi}{\partial y} \right)_\alpha + \left(\frac{\partial \varphi}{\partial y} \right)_p \tag{4}$$

where the subscript 2 refers to the tip, the subscripts α and p denote lift and roll, respectively, and φ is the linearized velocity potential. For streamwise-tip wings with subsonic leading edges and

supersonic trailing edges, equations for the potentials $(\varphi)_\alpha$ and $(\varphi)_p$ are derived in reference 11. These potentials were based on an approximation to the exact linearized solution (see reference 11) and rendered results therein that were in good agreement with computations based on a more exact analysis. It appears reasonable to assume, therefore, that for purposes of the present investigation the use of these potentials will lead to results that are of satisfactory accuracy.

The potentials (valid for the wing region between the right tip and the tip Mach line) are as follows:

$$(\varphi)_\alpha = \frac{2V\alpha\sqrt{2}}{\pi}\sqrt{\frac{(By + mx)(b - 2y)}{B(1 + m)}} \tag{5}$$

$$(\varphi)_p = \frac{p\sqrt{2}\left[2yB(2m + 1) + bB(m + 1) - 2mx\right]}{3\pi\left[(1 + m)B\right]^{3/2}}\sqrt{(By + mx)(b - 2y)} \tag{6}$$

Corresponding expressions for the left wing-tip region are obtained by replacing y by $-y$ in equations (5) and (6) and multiplying the right-hand side of equation (6) by the quantity -1. Inasmuch as $(\varphi)_\alpha$ is symmetrical and $(\varphi)_p$ antisymmetrical with respect to the x-axis it is sufficient to work with the right half-wing (equations (5) and (6)) and use the appropriate sign for the left half-wing.

Differentiation with respect to y yields

$$\left(\frac{\partial\varphi}{\partial y}\right)_\alpha = \frac{-V\alpha\sqrt{2}}{\pi\sqrt{B(1 + m)}}\left[\frac{2mx + 4By - bB}{\sqrt{(By + mx)(b - 2y)}}\right] \tag{7}$$

and

$$\left(\frac{\partial\varphi}{\partial y}\right)_p = \frac{p\sqrt{2}}{3\pi\left[(1 + m)B\right]^{3/2}}\left\{2B(2m + 1)\sqrt{(By + mx)(b - 2y)} - \left[2yB(2m + 1) + bB(m + 1) - 2mx\right]\left[\frac{4By + 2mx - bB}{2\sqrt{(By + mx)(b - 2y)}}\right]\right\} \tag{8}$$

Substitution of equations (7) and (8) in equation (4) and evaluation of the resultant expression for v_n in the immediate vicinity of the tip $\left(\text{i.e., } |y| \to \frac{b}{2}\right)$ yields

$$\left(v_{n_2}\right)_{|y| \to \frac{b}{2}} = -\frac{1}{\sqrt{\frac{b}{2} - |y|}} \left\{ \pm \frac{V\alpha\sqrt{2}\sqrt{bB + 2mx}}{\pi\sqrt{B(1 + m)}} + \frac{p(3mbB + 2bB - 2mx)\sqrt{bB + 2mx}}{3\pi\sqrt{2}\left[B(1 + m)\right]^{3/2}} \right\} \tag{9}$$

where the plus sign is to be used for the right edge and the minus sign for the left edge.

Equation (9) is seen to have the same form as equation (1) and, therefore, the suction force per unit length along the wing tip may be obtained from equation (2). For a streamwise tip, $M_n = 0$ and the suction force is expressible as

$$F_2 = \frac{\rho(Bb + 2mx)}{2\pi B(1 + m)} \left[4V^2\alpha^2 \pm \frac{4V\alpha p(3mbB + 2bB - 2mx)}{3B(1 + m)} + \frac{p^2(3mbB + 2bB - 2mx)^2}{9B^2(1 + m)^2} \right] \tag{10}$$

In equation (10) only the term

$$\pm \frac{2V\alpha p(3mbB + 2bB - 2mx)\rho(Bb + 2mx)}{3\pi B^2(1 + m)^2}$$

will give rise to a lateral force and a yawing moment; the force and moment are obtained by integrating this term along the wing tips. Inasmuch as the other terms of equation (10) have the same sign for both the left and the right wing tips, the net contribution of these terms to the lateral force and yawing moment of the wing will be zero.

Applications of equations (3) and (10) to the derivation of the stability derivatives C_{Y_p} and C_{n_p} are given in the following sections.

Stability Derivative C_{Y_p}

The lateral component of the suction force along the leading edge is expressible as follows (see reference 4):

$$Y_1 = \int_0^{\frac{b}{2}\tan\Lambda} \left(F_{1,R} - F_{1,L}\right)dx$$

$$= \frac{\pi\rho\sqrt{1 - m^2}(\cot^2\Lambda)\alpha V p I(m)}{E\left(\sqrt{1 - m^2}\right)} \int_0^{\frac{b}{2}\tan\Lambda} x^2 dx$$

$$= \frac{\pi}{24} b^3 \rho\alpha V p (\tan\Lambda) \frac{I(m)\sqrt{1 - m^2}}{E\left(\sqrt{1 - m^2}\right)} \tag{11}$$

where the subscripts R and L refer to the right edge and left edge, respectively. The lateral force coefficient is formed by division by $\frac{1}{2}\rho V^2 S$ and the derivative with respect to $\left(\frac{pb}{2V}\right)_{\frac{pb}{2V}\to 0}$ is the stability derivative C_{Y_p}. Thus

$$\left(C_{Y_p}\right)_1 = \left(\frac{\partial}{\partial\frac{pb}{2V}} \frac{Y_1}{\frac{1}{2}\rho V^2 S}\right)_{\frac{pb}{2V}\to 0}$$

$$= \frac{\pi\alpha AB}{6m} \frac{I(m)\sqrt{1 - m^2}}{E\left(\sqrt{1 - m^2}\right)}$$

or

$$\left(\frac{C_{Y_p}}{\alpha}\right)_1 = \frac{\pi AB}{6m} J(m) \tag{12}$$

The lateral force due to the suction along the tips is

$$Y_2 = \int_{Tip} \left(F_{2,R} - F_{2,L}\right) dx$$

$$= \frac{4\rho V \alpha p}{3\pi B^2 (1 + m)^2} \int_{bB/2m}^{\frac{bB}{2m}(1+\lambda\omega)} (3mbB + 2bB - 2mx)(bB + 2mx)dx$$

$$= \frac{\rho V \alpha p b^3 B^3 \lambda\omega}{9\pi B^2 (1 + m)^2 m} \left[12(3m + 1) + 3\lambda\omega(3m - 1) - 2\lambda^2\omega^2\right] \tag{13}$$

Converting to derivative form in terms of the parameters m, AB, and λ yields

$$\left(\frac{C_{Y_p}}{\alpha}\right)_2 = \frac{64\lambda}{9\pi(1 + \lambda)} \left\{ \frac{3(3m + 1)\left[AB(1 + \lambda)\right]^2 + 3\lambda m(3m - 1)\left[AB(1 + \lambda)\right] - 8\lambda^2 m^2}{\left[AB(1 + \lambda)(1 + m)\right]^2} \right\} \tag{14}$$

The derivative for the complete wing is obtained by adding the components given by equations (12) and (14), that is,

$$\frac{C_{Y_p}}{\alpha} = \left(\frac{C_{Y_p}}{\alpha}\right)_1 + \left(\frac{C_{Y_p}}{\alpha}\right)_2 \tag{15}$$

The expressions for the derivative C_{Y_p} have been derived relative to a system of body axes. Additional terms arising from a transformation to stability axes result in negligible changes in the derivative for small angles of attack. The derivative, therefore, may be considered satisfactory for either system of axes.

Stability Derivative C_{n_p}

The yawing moment of the leading-edge suction about the wing apex is expressible as (see reference 4)

$$N_{l_a} = -\int_0^{\frac{b}{2}\tan\Lambda} \left(F_{l,R} - F_{l,L}\right)\left(\csc^2\Lambda\right)x\,dx$$

$$= -\frac{\pi}{64}\rho\alpha V pb^4(\sec^2\Lambda)\frac{I(m)\sqrt{1 - m^2}}{E\left(\sqrt{1 - m^2}\right)} \qquad (16)$$

(The minus sign for the moment indicates counterclockwise rotation.)

The yawing-moment coefficient is formed by division by $\frac{1}{2}\rho V^2 Sb$ and the derivative with respect to $\left(\frac{pb}{2V}\right)_{\frac{pb}{2V}\to 0}$ is the stability derivative C_{n_p}. Thus

$$\left(C_{n_p}\right)_{l_a} = \left(\frac{\partial}{\partial\frac{pb}{2V}}\frac{N_{l_a}}{\frac{1}{2}\rho V^2 Sb}\right)_{\frac{pb}{2V}\to 0}$$

$$= -\frac{\pi\alpha AB}{16}\left(\frac{B}{m^2} + \frac{1}{B}\right)\frac{I(m)\sqrt{1 - m^2}}{E\left(\sqrt{1 - m^2}\right)}$$

or

$$\left(\frac{C_{n_p}}{\alpha}\right)_{1a} = -\frac{\pi AB}{16}\left(\frac{B}{m^2} + \frac{1}{B}\right)J(m) \tag{17}$$

The yawing moment due to the suction force along the tips is

$$N_{2a} = -\int_{Tip}\left(F_{2,R} - F_{2,L}\right)x\,dx$$

$$= -\frac{4\rho V\alpha p}{3\pi B^2(1+m)^2}\int_{bB/2m}^{\frac{bB}{2m}(1+\lambda\omega)}(3mbB + 2bB - 2mx)(bB + 2mx)x\,dx$$

$$= -\frac{\rho V\alpha p b^4 B^4 \lambda\omega}{36\pi B^2(1+m)^2m^2}\left[24(3m+1) + 6m\lambda\omega(2\lambda\omega + 9) - \lambda\omega(3\lambda^2\omega^2 + 8\lambda\omega - 6\right] \tag{18}$$

Converting to derivative form in terms of the parameters m, AB, B, and λ yields

$$\left(\frac{C_{n_p}}{\alpha}\right)_{2a} = -\frac{32\lambda B}{9\pi m(1+m)^2(1+\lambda)\left[AB(1+\lambda)\right]^3}\left\{3(3m+1)\left[AB(1+\lambda)\right]^3 + \right.$$

$$\left. 3m\lambda(1+9m)\left[AB(1+\lambda)\right]^2 + 8m^2\lambda^2(3m-2)\left[AB(1+\lambda)\right] - 24m^3\lambda^3\right\} \tag{19}$$

The derivative for the complete wing is obtained by adding the components given by equations (17) and (19), that is,

$$\left(\frac{C_{n_p}}{\alpha}\right)_a = \left(\frac{C_{n_p}}{\alpha}\right)_{1a} + \left(\frac{C_{n_p}}{\alpha}\right)_{2a} \tag{20}$$

The expressions for the derivative $\left(C_{n_p}\right)_a$ have been derived relative to a system of body axes with moments taken about the wing apex. To transform the moment reference to an arbitrary point located at a distance from the wing apex equal to h (measured in root chords) the following equation may be used:

$$C_{n_p} = \left(C_{n_p}\right)_a \pm \frac{hc_r}{b} C_{Y_p}$$

or for the wings considered herein

$$C_{n_p} = \left(C_{n_p}\right)_a \pm \frac{2h}{A(1 + \lambda)} C_{Y_p} \tag{21}$$

(The plus sign is to be used when the new reference point is located rearward of the wing apex, the minus sign when the reference point is ahead of the wing apex.)

The expression for C_{n_p} given in equation (21) may be further utilized in transforming to the system of stability axes. If C_{n_p}' denotes the derivative relative to the stability system and C_{n_p} the quantity given by equation (21), the following relationship will render excellent accuracy for small angles of attack:

$$C_{n_p}' = C_{n_p} - \alpha\left(C_{l_p} - C_{n_r}\right) \tag{22}$$

Inasmuch as the present paper treats only the derivatives C_{Y_p} and C_{n_p}, estimates of the damping-in-roll derivative C_{l_p} and the damping-in-yaw derivative C_{n_r} must be obtained from other sources. Values of C_{l_p} for the wings considered herein may be readily obtained from reference 11. Corresponding calculations for the stability derivative C_{n_r} are unavailable, but the contribution of this term relative to C_{l_p} is small for most practical plan forms and thus may usually be neglected

in equation (22) without introducing a significant error in the value of the derivative C_{n_p}'. For wings of very low aspect ratio, however, C_{n_r} is appreciable and should not be neglected.

RESULTS AND DISCUSSION

Since the functions $E\left(\sqrt{1 - m^2}\right)$, $I(m)$, and $J(m)$ appear in the derivation of the stability derivatives, variations of these functions with the parameter m are presented in figure 3 for convenience in applying the final equations.

As stated previously, the equations were derived for wings with subsonic leading edges and supersonic trailing edges. For configurations where the trailing edge is "slightly" subsonic, the derived equations may be used to yield rough estimates of the derivatives although the effect of the subsonic trailing edge has been neglected. For conditions where the trailing-edge Mach line intersects the tip, that is,

$$\frac{BA(1 + \lambda)}{4 + BA(1 + \lambda)} < B \cot \Lambda < \frac{BA(1 + \lambda)}{BA(1 + \lambda) + 4(1 - \lambda)}$$

the error introduced by neglecting the subsonic-edge effect is less than the error for conditions where the Mach line intersects the leading edge, that is,

$$B \cot \Lambda < \frac{BA(1 + \lambda)}{4 + BA(1 + \lambda)}$$

The error may be quite appreciable for many combinations of Mach number and plan-form parameters. Accordingly, extreme caution should be exercised in interpreting the rough estimates obtained for subsonic-trailing-edge plan forms.

Design-chart calculations (computed from equation (15)) for the derivative C_{Y_p} are presented in figure 4 in terms of the parameters AB, $B \cot \Lambda$, and λ. Dashed boundary lines are drawn to indicate regions of different trailing-edge conditions wherever feasible (i.e., figs. 4(b) to 4(e)). Inasmuch as a single curve was sufficient to present results

for $\lambda = 0$ (fig. 4(a)), boundary lines could not be indicated (since they are a function of the parameter AB). For convenience, the mathematical relationship governing the edge condition is presented in the figure.

Design-chart calculations for the derivative C_{n_p} relative to body axes with moments taken about the wing apex are presented in figures 5 and 6. For convenience of presentation, the derived expression for C_{n_p} (equation (20)) has been subdivided into three components $\left(C_{n_p}\right)_{aA}$, $\left(C_{n_p}\right)_{aB}$, and $\left(C_{n_p}\right)_{aC}$. Figure 5 presents the components $\left(C_{n_p}\right)_{aA}$ and $\left(C_{n_p}\right)_{aB}$ both of which are independent of taper ratio; figure 6 presents the component $\left(C_{n_p}\right)_{aC}$. The derivative is obtained by summing the components, that is,

$$\left(C_{n_p}\right)_a = \left(C_{n_p}\right)_{aA} + \left(C_{n_p}\right)_{aB} + \left(C_{n_p}\right)_{aC} \tag{23}$$

As with the charts for C_{Y_p}, either dashed boundary lines or mathematical relationships are included in the figures to indicate regions of different trailing-edge conditions. It is noted that figure 6 does not include curves for $\lambda = 0$; the component $\left(C_{n_p}\right)_{aC}$ is zero for all wings of $\lambda = 0$ and hence may be disregarded in equation (23).

Some illustrative variations of the derivatives with Mach number, aspect ratio, taper ratio, and leading-edge sweepback are presented in figures 7 and 8. The derivatives are once again presented relative to body axes with moments taken about the wing apex. Caution must be exercised in interpreting these variations, however, inasmuch as the results and trends will depend on the system of axes used, the point about which moments are taken, and the specific plan form under consideration.

The data presented in the design charts and illustrative variations may be transformed to a stability-axes system with moments taken about an arbitrary point by use of equations (21) and (22).

CONCLUDING REMARKS

On the basis of the linearized theory for supersonic flow, the lateral force and yawing moment due to combined angle of attack and rolling have been evaluated for some families of sweptback tapered wings with streamwise tips and subsonic leading edges.

Results of the analysis are presented in the form of design charts which permit estimation of the stability derivatives C_{Y_p} and C_{n_p}. Some illustrative variations of the derivatives with aspect ratio, taper ratio, Mach number, and leading-edge sweep are also presented. All numerical data are presented relative to a body-axes system with moments taken about the wing apex. For convenience in application, formulas are given for transforming from this system to a stability-axes system with moments taken about an arbitrary point.

Langley Aeronautical Laboratory
National Advisory Committee for Aeronautics
Langley Air Force Base, Va., April 12, 1950

REFERENCES

1. Ribner, Herbert S.: The Stability Derivatives of Low-Aspect-Ratio Triangular Wings at Subsonic and Supersonic Speeds. NACA TN 1423, 1947.

2. Jones, Arthur L., and Alksne, Alberta: The Damping Due to Roll of Triangular, Trapezoidal, and Related Plan Forms in Supersonic Flow. NACA TN 1548, 1948.

3. Brown, Clinton E.: Theoretical Lift and Drag of Thin Triangular Wings at Supersonic Speeds. NACA Rep. 839, 1946.

4. Ribner, Herbert S., and Malvestuto, Frank S., Jr.: Stability Derivatives of Triangular Wings at Supersonic Speeds. NACA Rep. 908, 1948.

5. Malvestuto, Frank S., Jr., and Margolis, Kenneth: Theoretical Stability Derivatives of Thin Sweptback Wings Tapered to a Point with Sweptback or Sweptforward Trailing Edges for a Limited Range of Supersonic Speeds. NACA TN 1761, 1949.

6. Harmon, Sidney M.: Stability Derivatives at Supersonic Speeds of Thin Rectangular Wings with Diagonals ahead of Tip Mach Lines. NACA Rep. 925, 1949.

7. Jones, Arthur L., and Alksne, Alberta: The Yawing Moment Due to Sideslip of Triangular, Trapezoidal, and Related Plan Forms in Supersonic Flow. NACA TN 1850, 1949.

8. Brown, Clinton E., and Adams, Mac C.: Damping in Pitch and Roll of Triangular Wings at Supersonic Speeds. NACA Rep. 892, 1948.

9. Margolis, Kenneth: Theoretical Lift and Damping in Roll of Thin Sweptback Tapered Wings with Raked-In and Cross-Stream Wing Tips at Supersonic Speeds. Subsonic Leading Edges. NACA TN 2048, 1950.

10. Jones, Arthur L: The Theoretical Lateral-Stability Derivatives for Wings at Supersonic Speeds. Jour. Aero. Sci., vol. 17, no. 1, Jan. 1950, pp. 39-46.

11. Malvestuto, Frank S., Jr., Margolis, Kenneth, and Ribner, Herbert S: Theoretical Lift and Damping in Roll of Thin Sweptback Wings of Arbitrary Taper and Sweep at Supersonic Speeds. Subsonic Leading Edges and Supersonic Trailing Edges. NACA TN 1860, 1949.

12. Harmon, Sidney M., and Jeffreys, Isabella: Theoretical Lift and Damping in Roll of Thin Wings with Arbitrary Sweep and Taper at Supersonic Speeds. Supersonic Leading and Trailing Edges. NACA TN 2114, 1950.

13. Cohen, Doris: The Theoretical Lift of Flat Swept-Back Wings at Supersonic Speeds. NACA TN 1555, 1948.

14. Cohen, Doris: Theoretical Loading at Supersonic Speeds of Flat Swept-Back Wings with Interacting Trailing and Leading Edges. NACA TN 1991, 1949.

15. Walker, Harold J., and Ballantyne, Mary B.: Pressure Distribution and Damping in Steady Roll at Supersonic Mach Numbers of Flat Swept-Back Wings with Subsonic Edges. NACA TN 2047, 1950.

16. Von Kármán, Th., and Burgers, J. M.: General Aerodynamic Theory - Perfect Fluids. Theory of Airplane Wings of Infinite Span. Vol. II of Aerodynamic Theory, div. E, ch. II, sec. 10, W. F. Durand, ed., Julius Springer (Berlin), 1935, pp. 48-53.

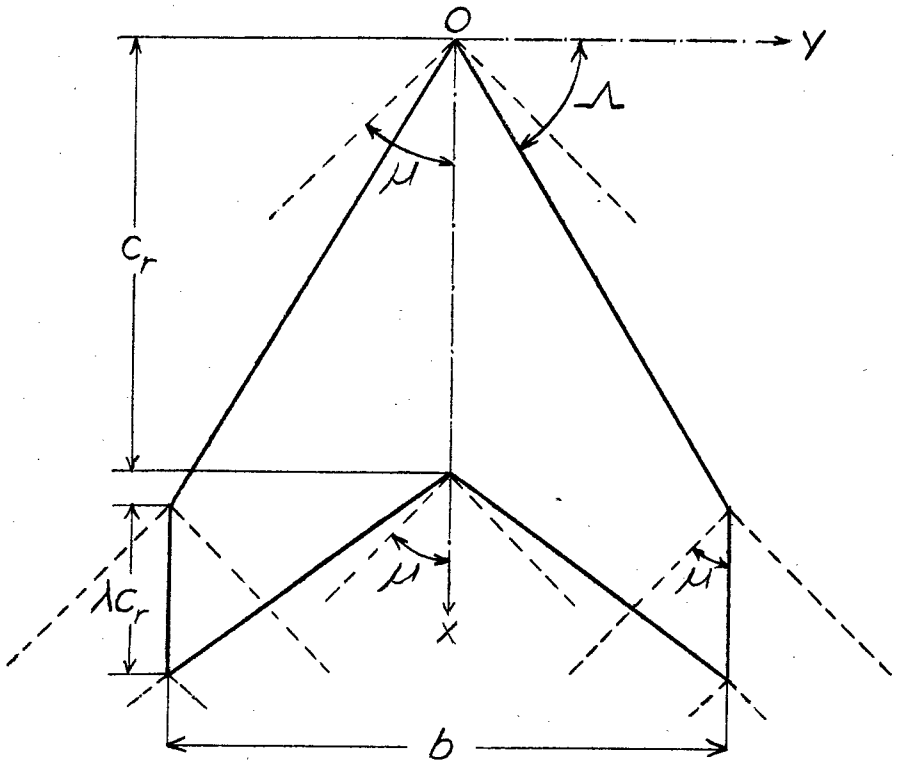

(a) Sweptback trailing edge.

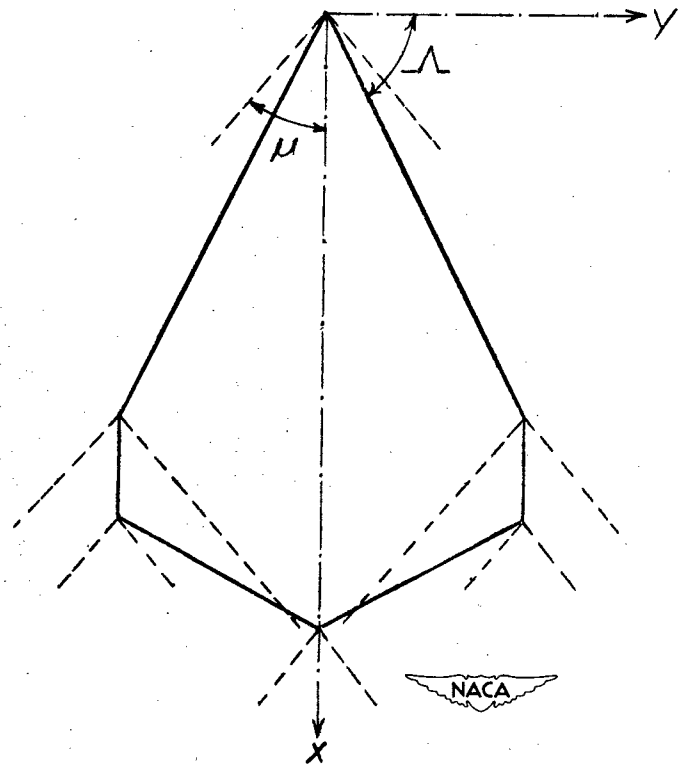

(b) Sweptforward trailing edge.

Figure 1.- Sweptback wings considered in the analysis.

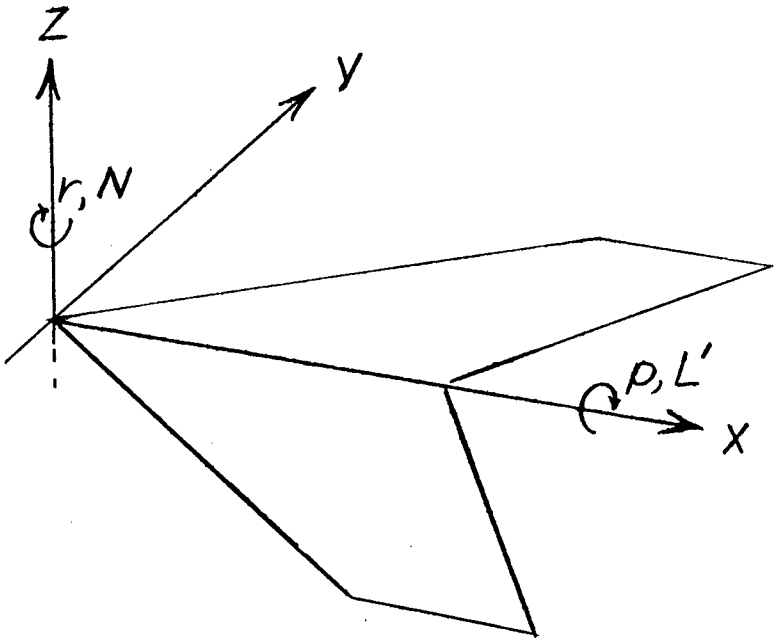

(a) Body axes used in analysis.

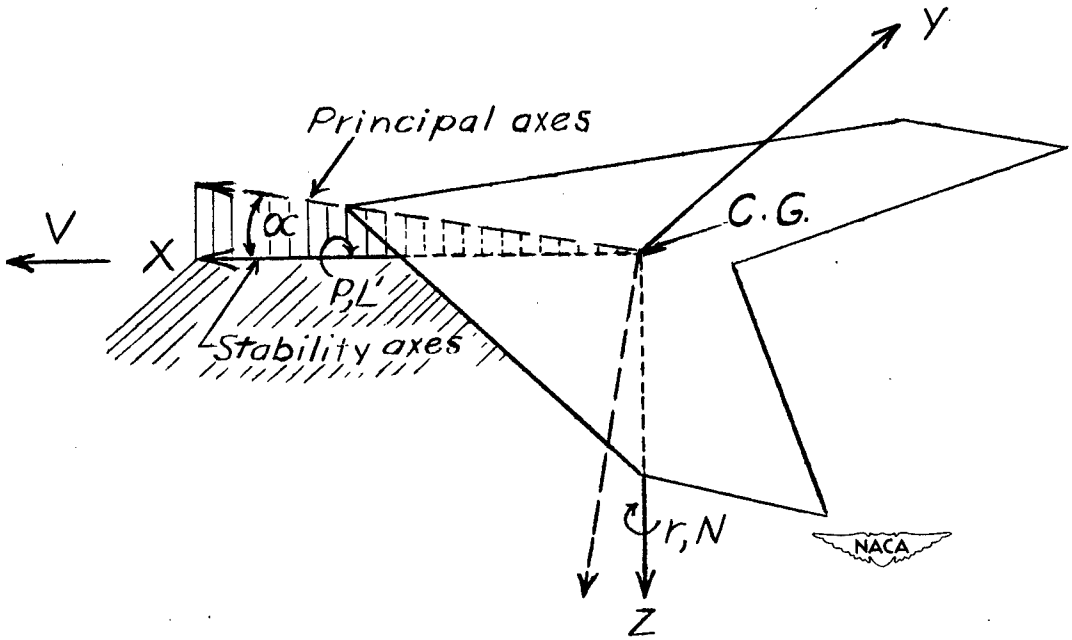

(b) Stability axes. Velocity, force, and moment arrangement in principal body-axes system is identical to that of stability-axes system. (Principal body axes dashed in for comparison.)

Figure 2.- System of axes and associated data.

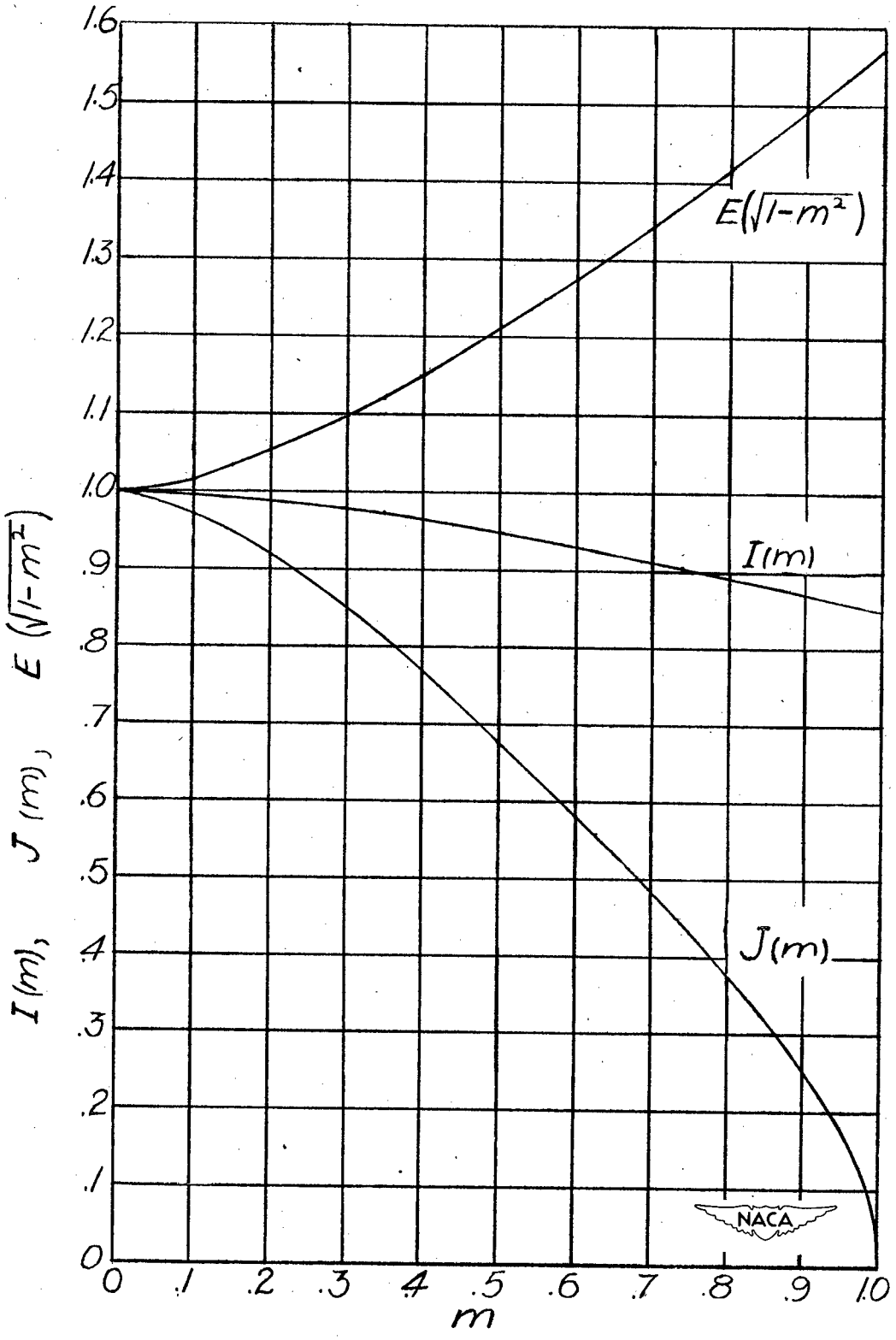

Figure 3.- Variation of the elliptic integral factors with m.

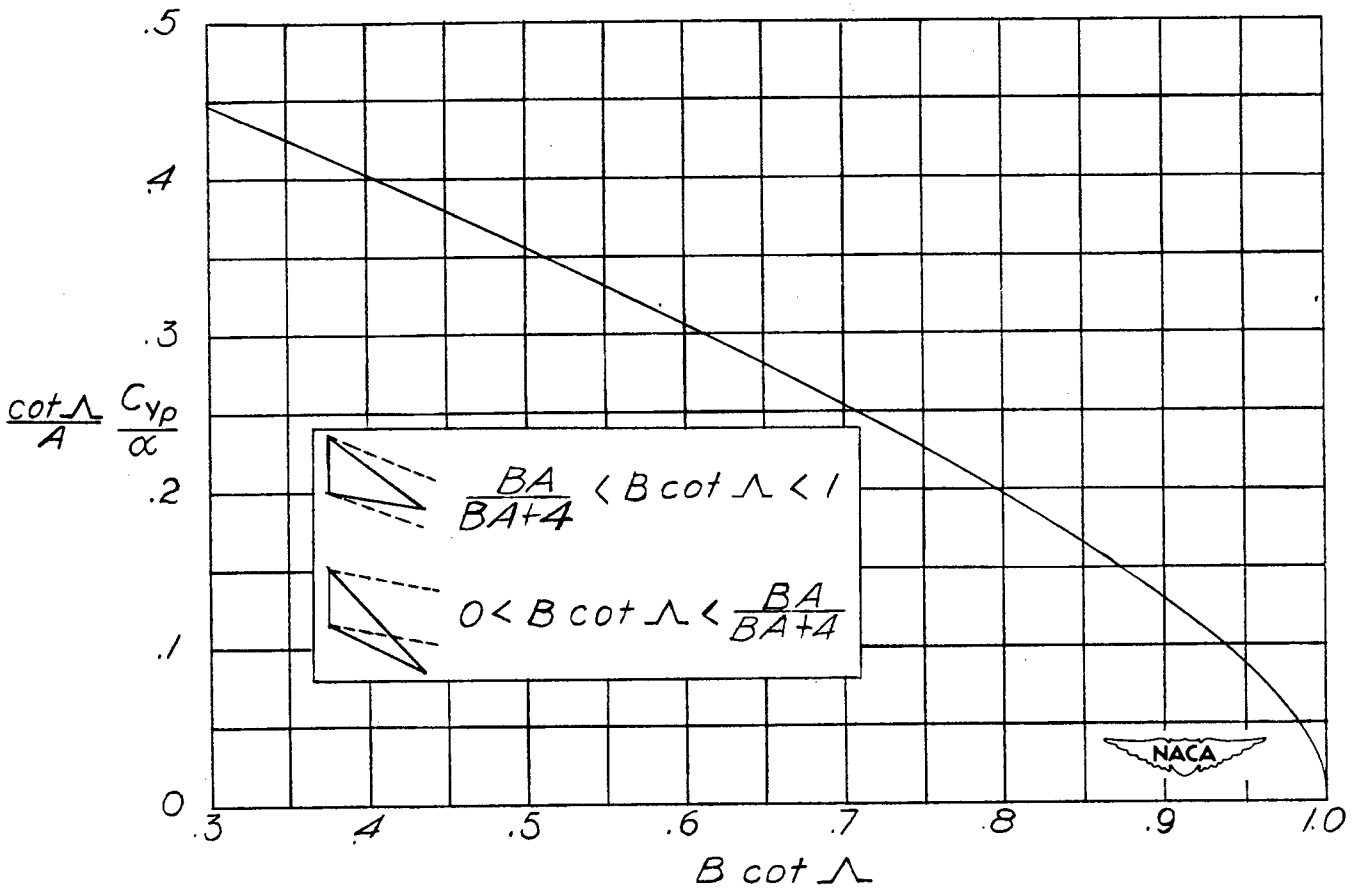

(a) $\lambda = 0$.

Figure 4.- Variations of the stability derivative C_{Y_p} with the parameter B cot Λ. (Results are valid for either body or stability system of axes; α is measured in radians. Data for plan forms with subsonic trailing edges have limited significance - see section of text entitled "Results and Discussion.")

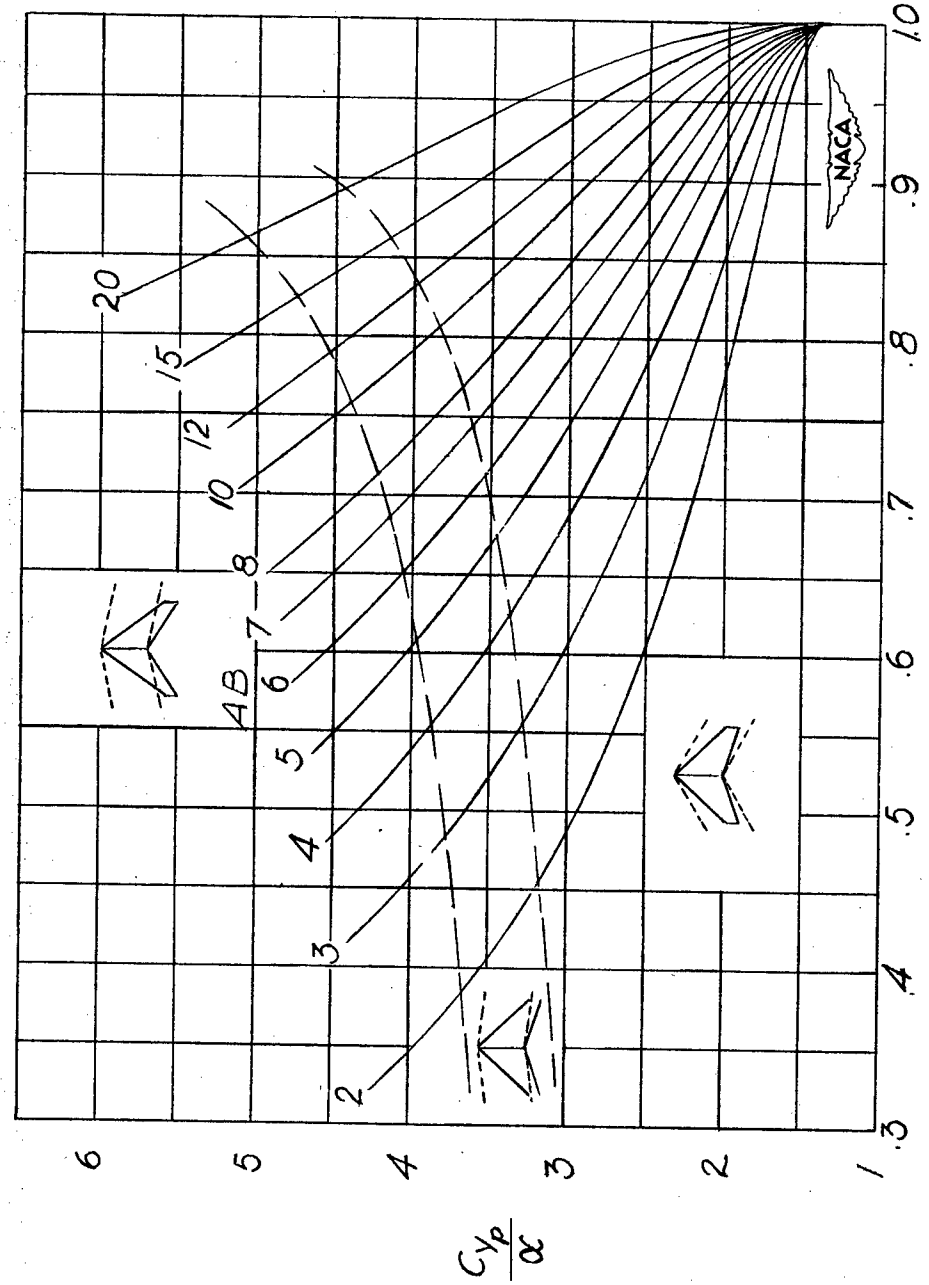

(b) $\lambda = 0.25$.

Figure 4.- Continued.

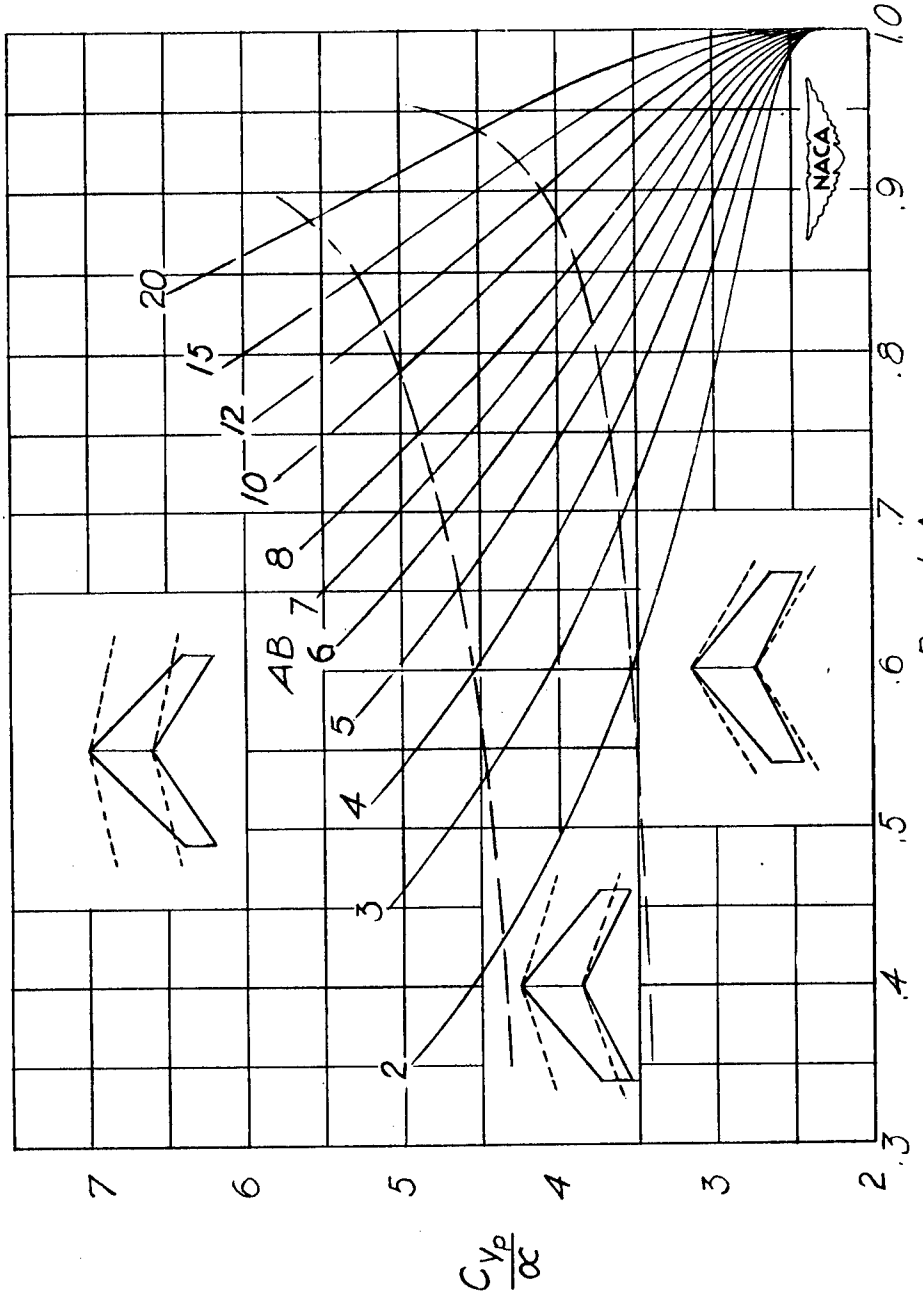

(c) $\lambda = 0.50$.

Figure 4.- Continued.

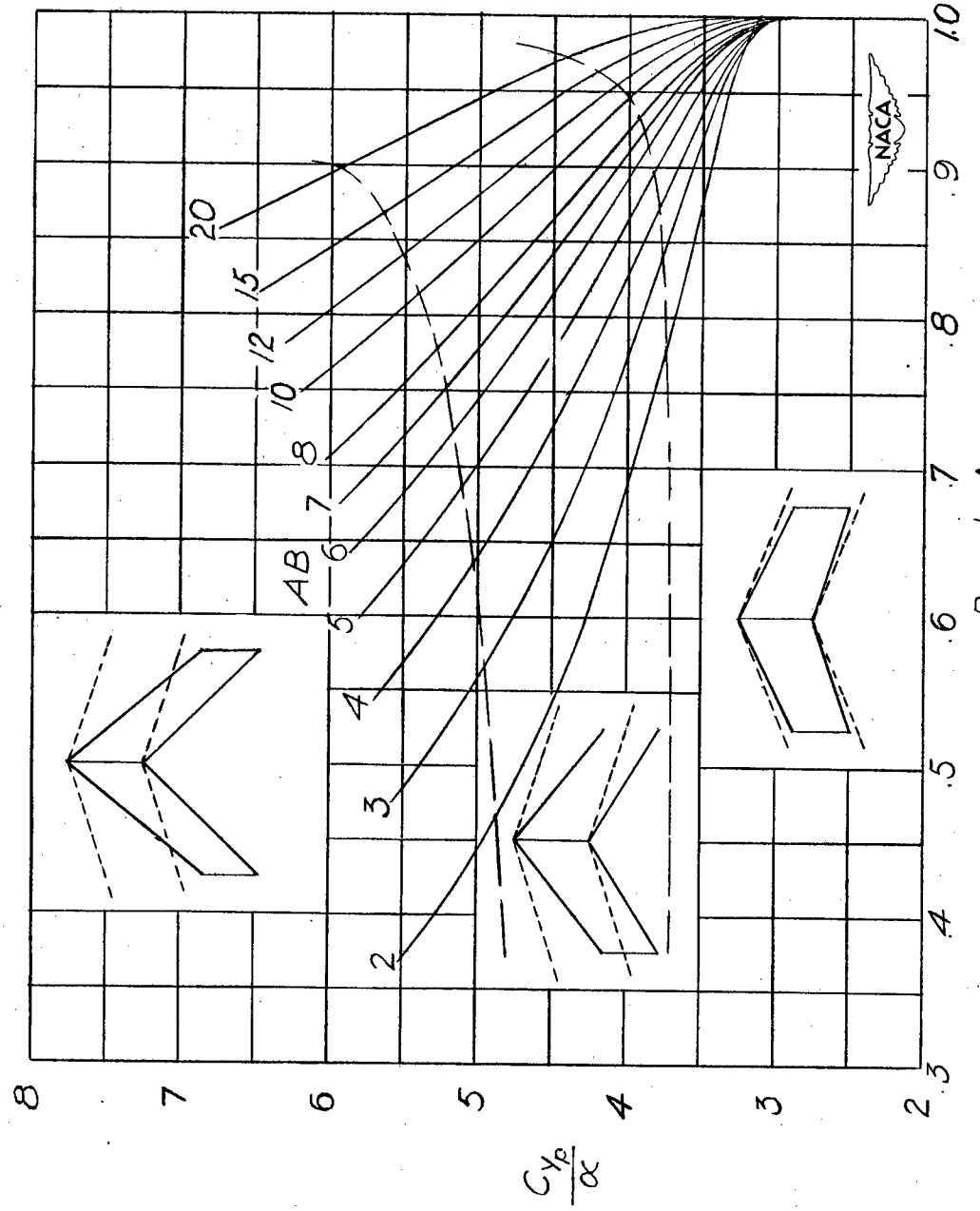

(d) $\lambda = 0.75$.

Figure 4.- Continued.

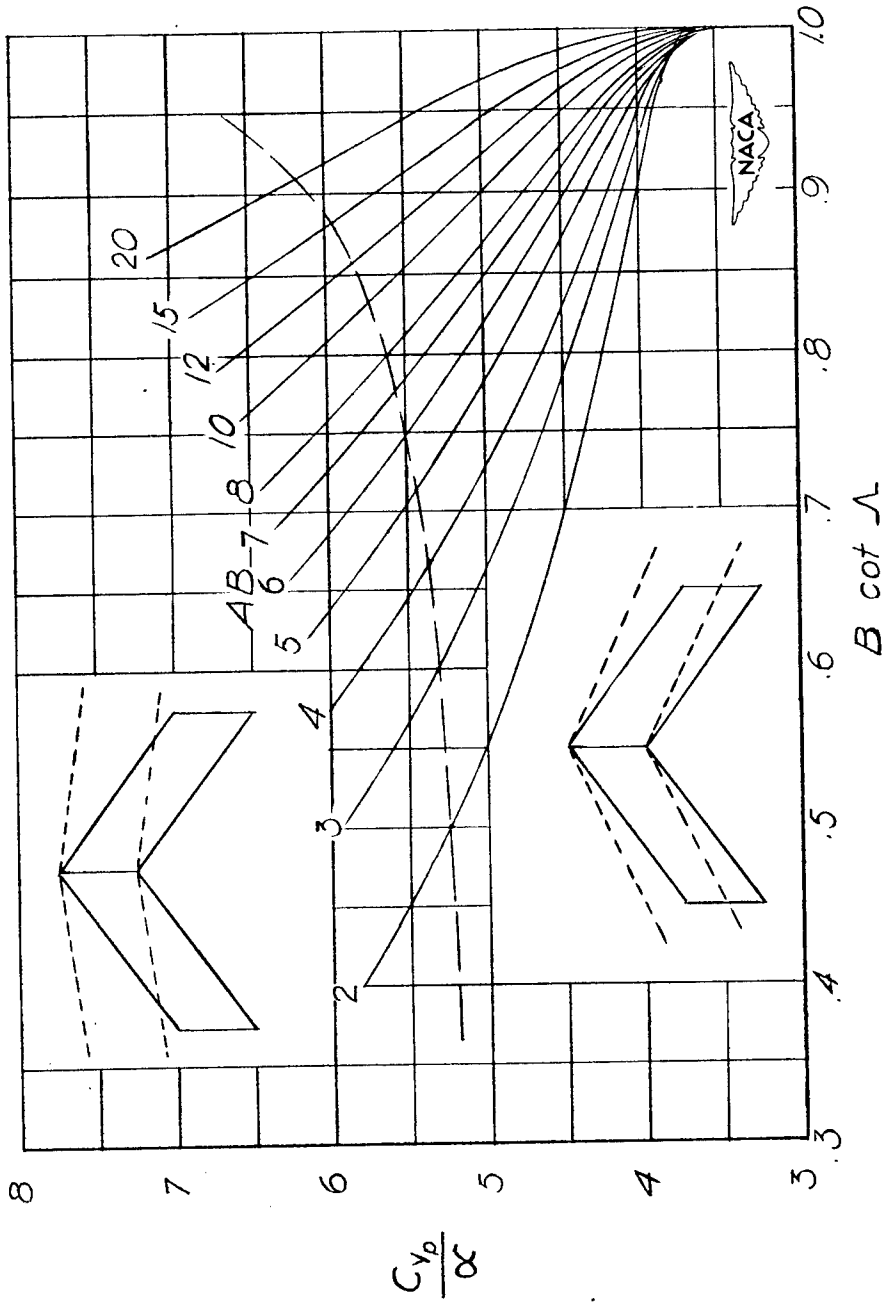

(e) $\lambda = 1.00$.

Figure 4.- Concluded.

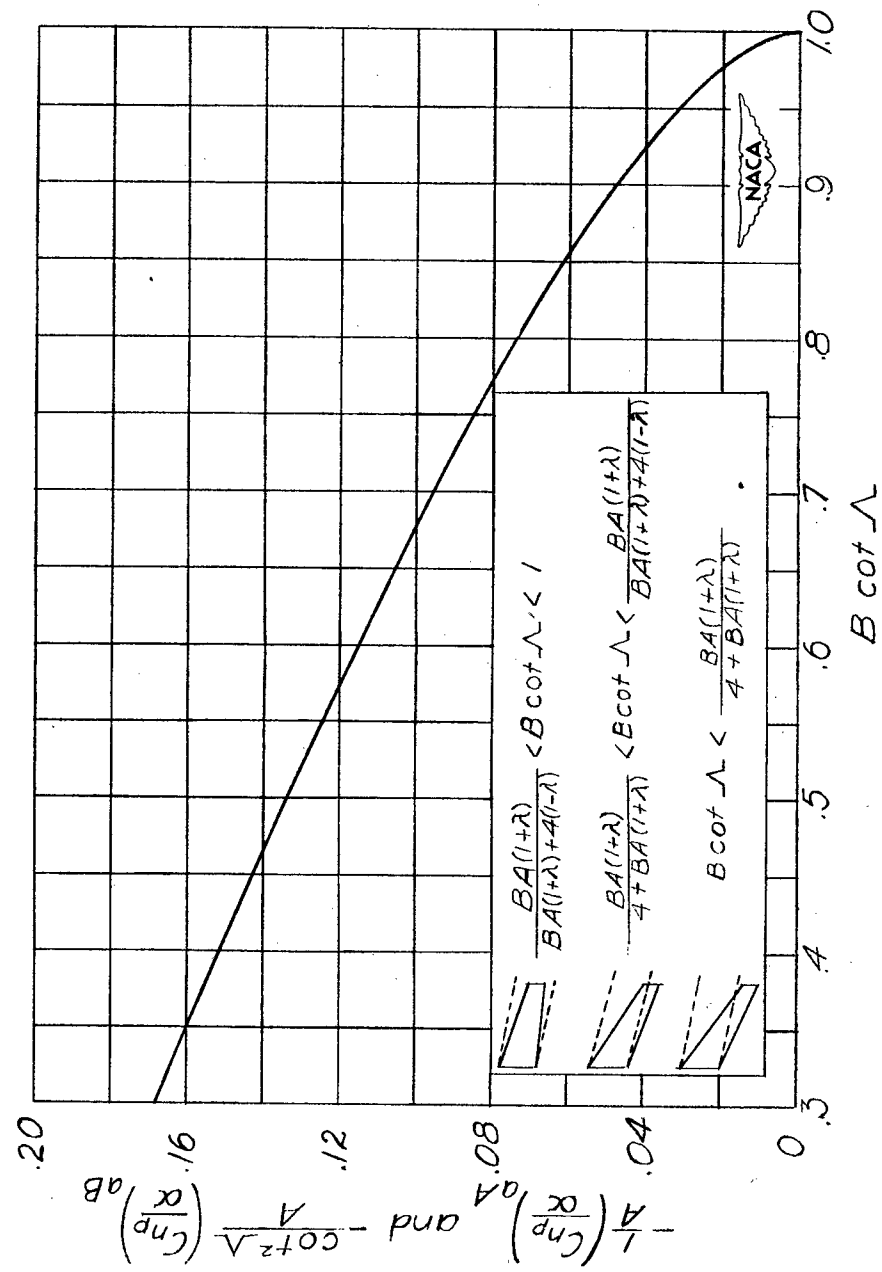

Figure 5.- Variations of the stability-derivative components $(C_{n_p})_{aA}$ and $(C_{n_p})_{aB}$ with the parameter B cot Λ. (Results are valid for a body-axes system with moments taken about the wing apex; α is measured in radians. Data for plan forms with subsonic trailing edges have limited significance - see section of text entitled "Results and Discussion.") $(C_{n_p})_a = (C_{n_p})_{aA} + (C_{n_p})_{aB} + (C_{n_p})_{aC}$.

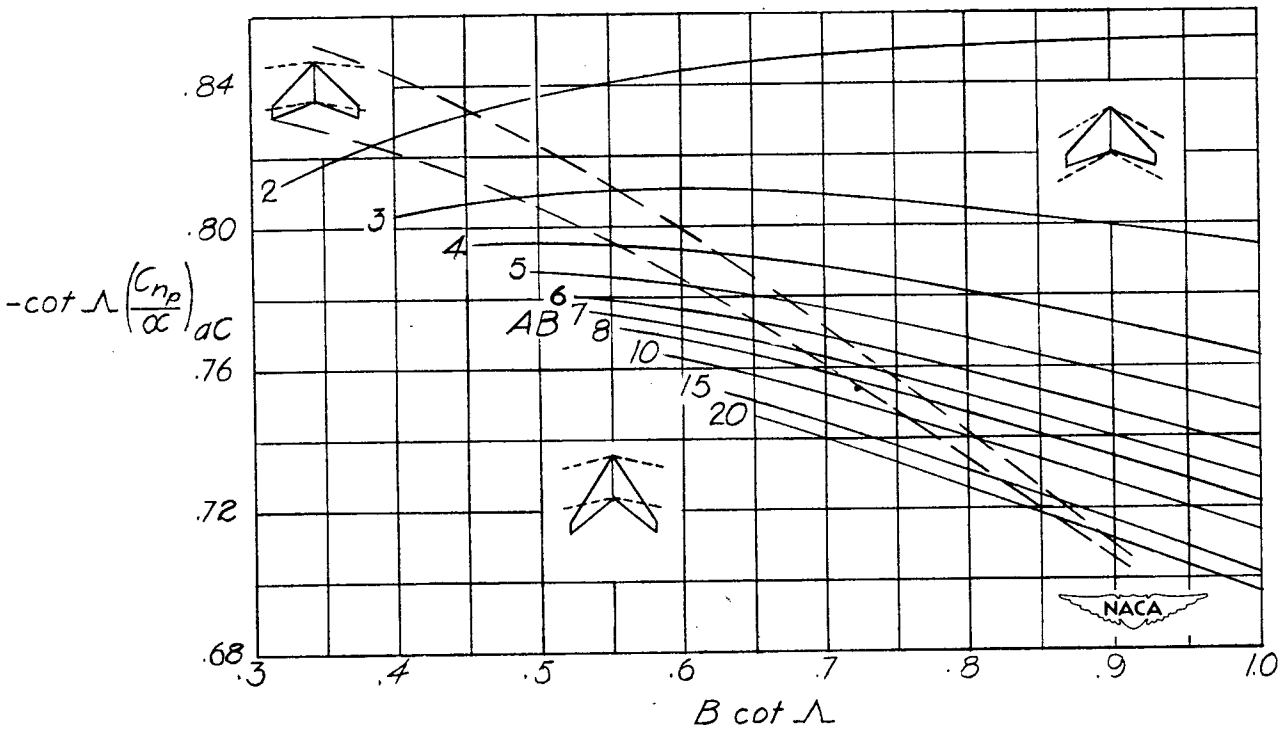

(a) $\lambda = 0.25$.

Figure 6.- Variations of the stability-derivative component $\left(C_{n_p}\right)_{aC}$ with the parameter B cot Λ. (Results are valid for a body-axes system with moments taken about the wing apex; α is measured in radians. Data for plan forms with subsonic trailing edges have limited significance - see section of text entitled "Results and Discussion.")

$\left(C_{n_p}\right)_a = \left(C_{n_p}\right)_{aA} + \left(C_{n_p}\right)_{aB} + \left(C_{n_p}\right)_{aC}$.

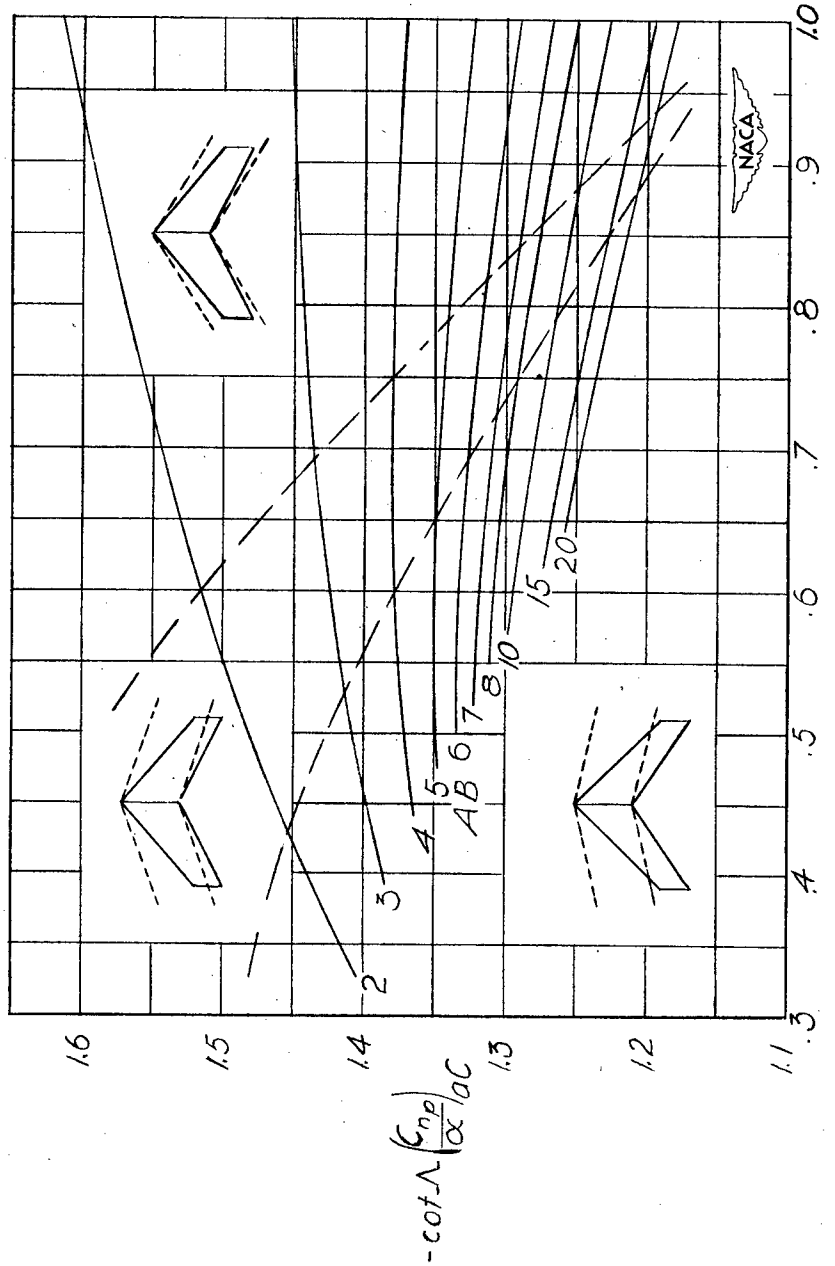

(b) $\lambda = 0.50$.

Figure 6.- Continued.

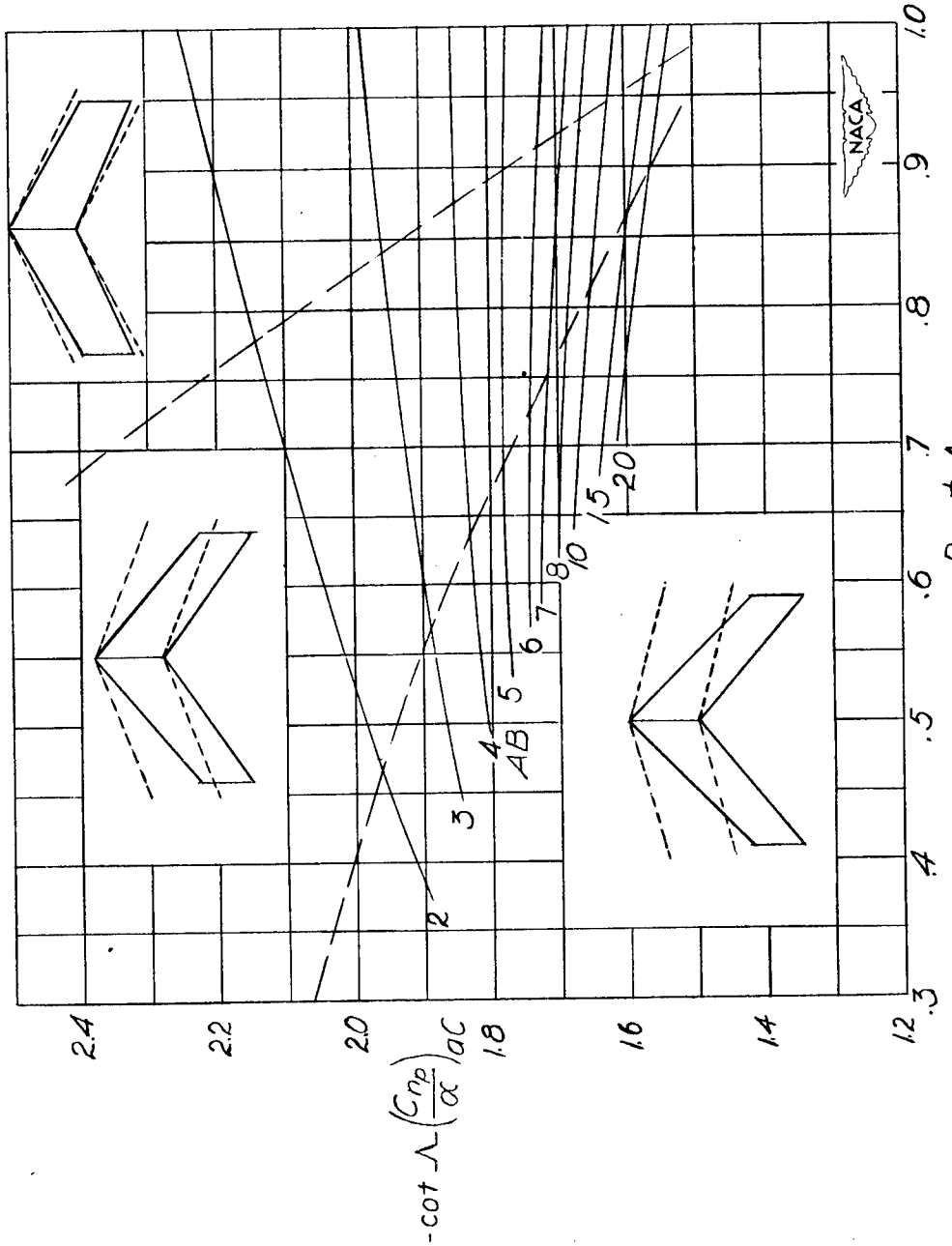

(c) $\lambda = 0.75$.

Figure 6.- Continued.

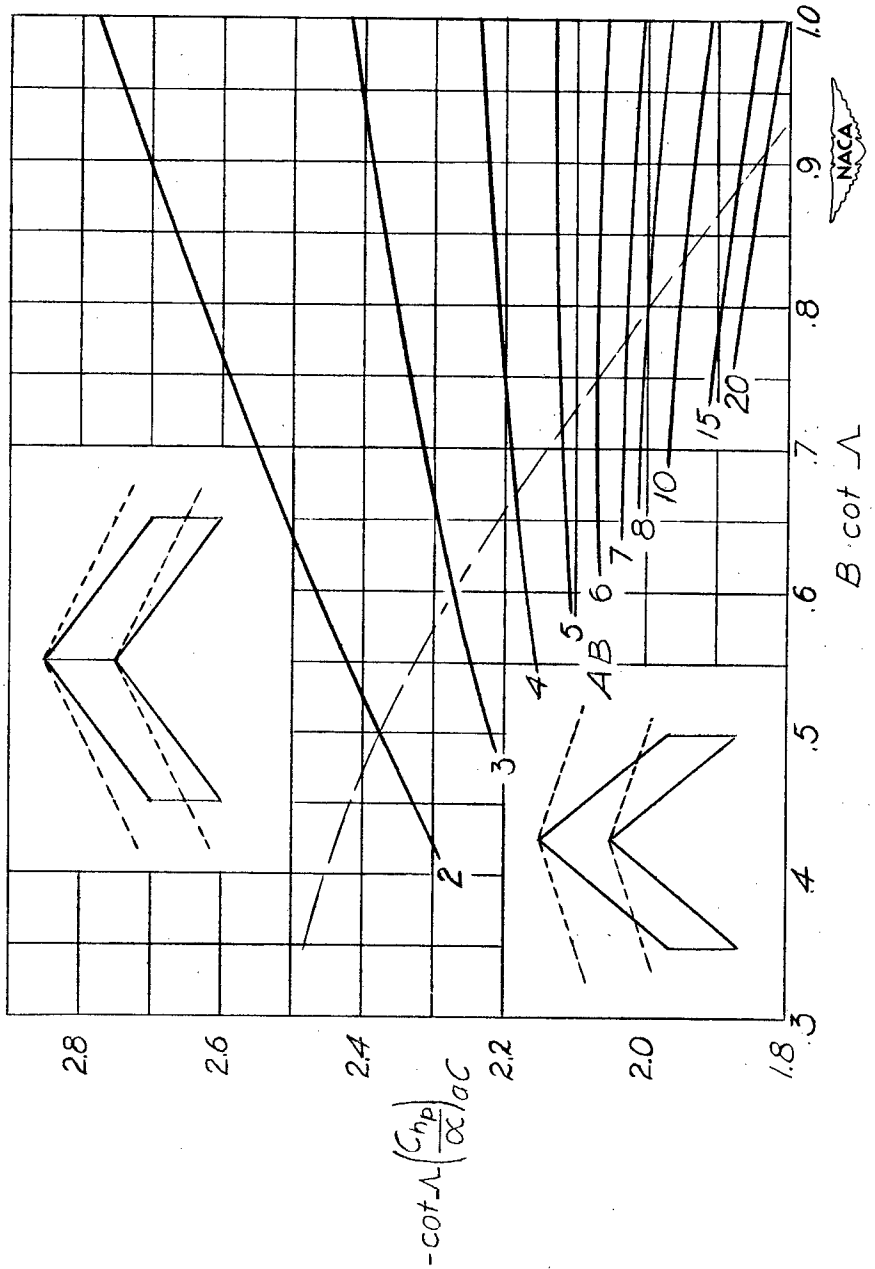

(d) $\lambda = 1.00$.

Figure 6.- Concluded.

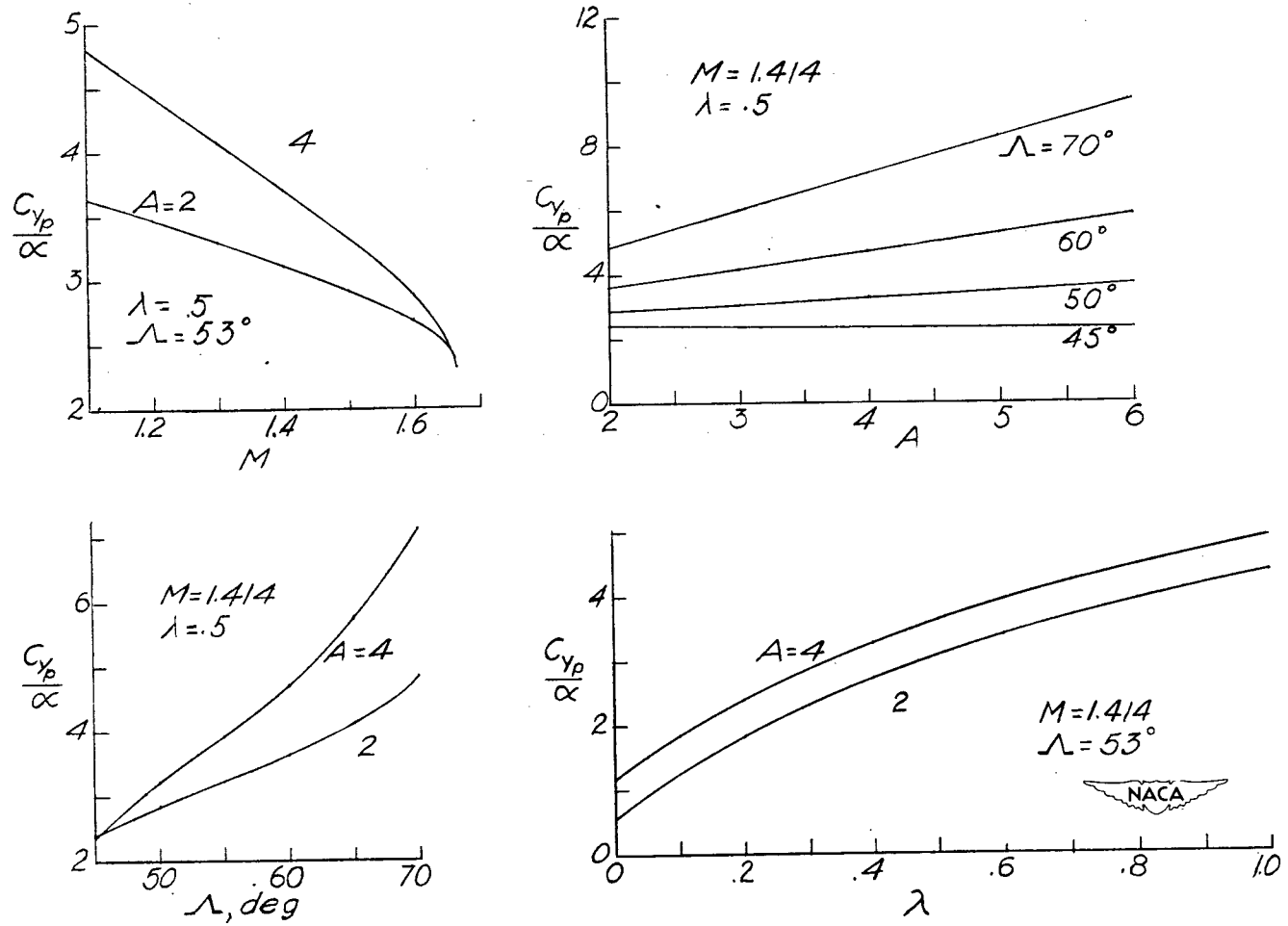

Figure 7.- Some illustrative variations of the stability derivative C_{Y_p} with Mach number, aspect ratio, leading-edge sweepback, and taper ratio. (Results are valid for either body or stability system of axes; α is measured in radians.)

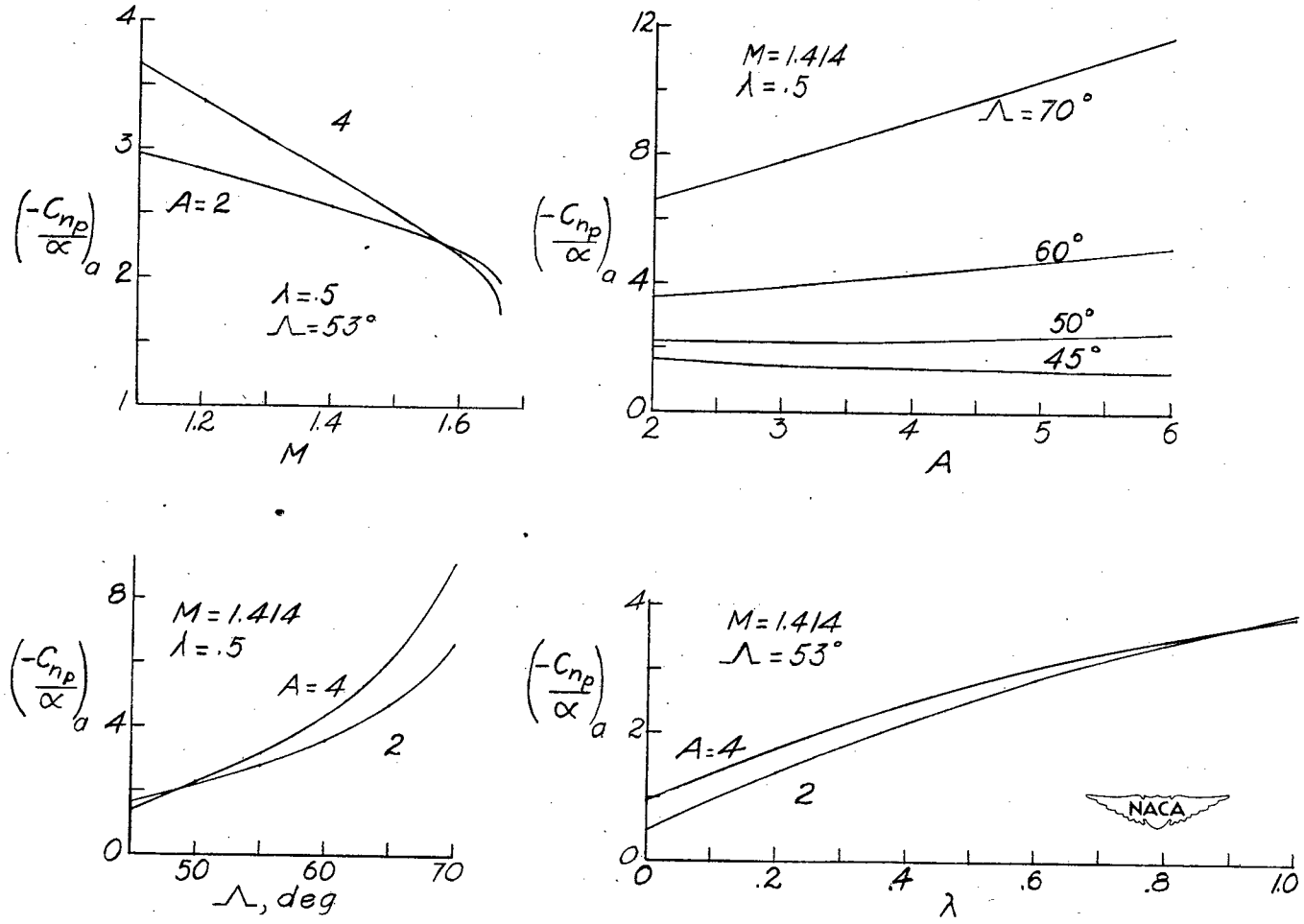

Figure 8.- Some illustrative variations of the stability derivative C_{n_p} with Mach number, aspect ratio, leading-edge sweepback, and taper ratio. (Results are valid for a body system of axes with moments taken about the wing apex; α is measured in radians.)